Saudi Pharmaceutical Journal 31 (2023) 815–823

HOSTED BY

Contents lists available at ScienceDirect

Saudi Pharmaceutical Journal

journal homepage: www.sciencedirect.com

Original article

Benzo[g]quinazolines as antifungal against candidiasis: Screening, molecular docking, and QSAR investigations

Hatem A. Abuelizz [a,*], Ahmed H. Bakheit [a], Mohamed H. Al-Agamy [b], Harunor Rashid [c], Gamal A.E. Mostafa [a], Rashad Al-Salahi [a,*]

[a] Department of Pharmaceutical Chemistry, College of Pharmacy, King Saud University, Riyadh 11451, Saudi Arabia
[b] Department of Pharmaceutics, College of Pharmacy, King Saud University, Riyadh 11451, Saudi Arabia
[c] National Centre for Immunisation Research and Surveillance (NCIRS), Kids Research at The Children's Hospital, Faculty of Medicine and Health, The University of Sydney, Westmead, NSW 2145, Australia

ARTICLE INFO

Article history:
Received 25 December 2022
Accepted 10 April 2023
Available online 15 April 2023

Keywords:
Anticandidal agent
Benzo[g]quinazolines
Candida albicans
CYP51
Molecular docking
Quantitative structure–activity relationship

ABSTRACT

Candida albicans, an opportunistic pathogen, is the most common type of fungus and represents a substantial source of human invasive disease (nosocomial infection). This category of fungi are part of our microbiota, and given the appropriate environmental conditions, it has the potential to cause both superficial and systemic infections. There is a soaring resistance against the available anticandidal agents. The purpose of this research is to investigate the activity of certain previously synthesized benzo[g]quinazolines against *C. albicans in vitro* by using the cup-plate diffusion method. There was a marked difference in the effectiveness of the target compounds **1–6** against the sample of *C. albicans* that was tested. Benzo[g]quinazolines **1** (inhibition zone = 20 mm) and **2** (inhibition zone = 22 mm) had good effects in comparison to fluconazole (inhibition zone = 26 mm). A docking study was conducted between benzo[g]quinazolines **1–6** and *Candida* spp. CYP51 to establish the binding mode compared with fluconazole and VT-1161 (oteseconazole) as reference medicines, and it was determined that binding at the active site of *Candida* spp. CYP51 occurred in the same manner. Quantitative structure–activity relationship (QSAR) investigation was performed to further characterize the identified anticandidal agents and recognize the major regulatory components governing such activity. In future studies, the benzo[g]quinazoline scaffold could serve as a model for the design and development of novel derivatives with antifungal potential.

© 2023 The Author(s). Published by Elsevier B.V. on behalf of King Saud University. This is an open access article under the CC BY-NC-ND license (http://creativecommons.org/licenses/by-nc-nd/4.0/).

1. Introduction

Candida albicans is considered to be a member of the human microflora (a diploid polymorphic yeast), and it is the form of fungus that is most commonly found on mucosal surfaces (Dadar et al., 2018; Nobile and Johnson, 2015; Turner and Butler, 2014). It colonizes the gastrointestinal, oral, skin, and genitourinary tracts of healthy bodies; however, in the presence of alterations in host immune response, such as stress or immunosuppressant administration, *C. albicans* can become an opportunistic organism and rapidly cause both systemic life-threatening and superficial candidiasis (Pfaller et al., 2011; Rothstein et al., 2001; Whaley et al., 2017). Globally, the emergence of *C. albicans* and non-*albicans* species (*C. glabrata*, *C. krusei*, *C. tropicalis*, and *C. parapsilosis*) plays a significant role in systemic infections (Conti et al., 2014; Turner and Butler, 2014). In addition to their obvious effects on superficial vaginal or oral mucosa, they may invade the bloodstream under favourable conditions and cause infections of deeper tissues (Conti et al., 2014; Turner and Butler, 2014; Whaley et al., 2017). It has been noticed that *C. albicans* systemic infections are associated with a mortality rate of 40% [8]; and *C. albicans* is responsible for 46.3% of all cases of invasive candidiasis, followed by *C. glabrata* and *C. parapsilosis* (24.4% & 8.1%)(Andes et al., 2016).

The severity of symptoms brought on by *C. albicans* infections is highly dependent on the host immune response and the

* Corresponding authors.
E-mail addresses: Habuelizz@ksu.edu.sa (H.A. Abuelizz), abujazz76@gmail.com (A.H. Bakheit), malagamy@ksu.edu.sa (M.H. Al-Agamy), harunor.rashid@health.nsw.gov.au (H. Rashid), gmostafa@ksu.edu.sa (G.A.E. Mostafa), ralsalahi@ksu.edu.sa (R. Al-Salahi).

Peer review under responsibility of King Saud University.

ELSEVIER Production and hosting by Elsevier

https://doi.org/10.1016/j.jsps.2023.04.012
1319-0164/© 2023 The Author(s). Published by Elsevier B.V. on behalf of King Saud University.
This is an open access article under the CC BY-NC-ND license (http://creativecommons.org/licenses/by-nc-nd/4.0/).

damaged organs or tissues. *C. albicans* infection is related to prior antifungal therapy, cardiac disease, neutropenia, lung disease, kidney disease, neurological disease, gastrointestinal disease, organ transplant, and human immunodeficiency virus (Whaley et al., 2017; Chandrika and Sharma, 2020). The cytochrome P450 superfamily includes the enzyme sterol 14-demethylase (CYP51), which plays a crucial role in the oxidation of the 14-methyl group in sterol precursors (Abuelizz,et al., 2021). The strongest fungicidal effects of sterols come from their production, and their capacity to activate nuclear receptors makes CYP51 an essential target for medications developed for the treatment of people, animals, and plants. Moreover, cholesterol production is also suppressed when human CYP51 is inhibited in patients being treated for CYP51 infections caused by fungi. In general, azoles are recognized as the best CYP51 inhibitors and are widely used in the medical, pharmaceutical, and agricultural fields as antifungals. As a result of their selectivity to inhibit the fungal CYP51 as opposed to the human ortholog, azoles are characterized as being more effective and safe agents. Azole drugs having greater affinity for fungal P450 enzymes over mammalian P450 enzymes, are used to treat systemic human infections. Econazole, miconazole, oxiconazole, etc. (bearing one nitrogen heterocycle) and clotrimazole, fluconazole, ketoconazole, etc. (bearing two or more nitrogen heterocycles) are antifungal agents used in clinical settings, however, they have limited effectiveness due to low systemic availability, potential drug-drug interactions, or increased resistance of fungal targets towards these drugs (Chandrika and Sharma, 2020).

Benzo[g]quinazolines have a variety of known biological activities (Abuelizz et al., 2018, 2020, 2021; Al-Salahi et al., 2019, 2018, 2017, 2016, 2015; Almehizi et al., 2019). In our previous work (Abuelizz et al., 2021), some benzo[g]quinazolines were identified as good agents against candidiasis (minimum inhibitory concentration $(MIC)_{50}$ = 0. 0.53 and 1.7 μg/ml) compared with the standard ketconazole (MIC_{50} = 0.45 μg/ml). As the incidence of invasive fungal infections, particularly in immunocompromised individuals, continues to rise, the demand for novel antifungal medicines is a major issue. The purpose of this work was to investigate the antifungal activity of the target benzo[g]quinazolines **1–6** against *C. albicans*, as well as the structural features responsible for this activity. The docking model was performed to assess the potential effects of target molecules **1–6** and sterol 14 α-demethylase (CYP51) in the binding pocket, as well as the interactions between benzo[g]quinazolines and amino acid residues in the active sites.

2. Materials and methods

2.1. Synthesis of the benzo[g]quinazolines *1–6*

The general processes for preparing compounds **1–6** have been previously documented (Al-Salahi et al., 2015, 2018a, 2019a; Abuelizz et al., 2020a, 2020b). Briefly, in triethyl amine (TEA) as a basic medium (3 mmol), the reaction of ethyl(phenethyl)isothio cyanate (1.5 mmol) and 3-amino-2-naphthaoic acid (1 mmol) under a refluxing condition in dimethyl formamide (DMF = 8 mL) for 3–5 h produced benzo[g]quinazolines **1** and **2** in good yields. The benzo[g]quinazolines **3–5** were obtained when compound **1** (1 mmol) or **2** (1 mmol) was treated with the appropriate alkyl/heteroalkyl halide (1.5 mmol) in the presence of a base as potassium carbonate (K_2CO_3 = 0.5 mmol) in DMF (8 mL) at 90 °C for 20 h. The reaction between **1** (1 mmol) and hydrazine hydate (0.5 mL) in boiling DMF (7 mL) for 15–18 h produced **6** (Al-Salahi et al., 2018a, 2019a; Abuelizz et al., 2020a, 2020b).

2.2. Antifungal screening

Antifungal activity for the compounds **1–6** are screened by the plate diffusion method using cup-plate diffusion and by determination of MIC according to the previously described methods (Wayne PA, 2009 and 2017).

2.2.1. Cup-plate diffusion method

Antifungal activity of the **1–6** compounds was determined using cup plate diffusion method according to the Clinical and Laboratory Standards Institute (CLSI) guidelines (Yousef et al., 2020). The benzoquinazolines **1–6** were dissolved in dimethyl sulfoxide (DMSO) to a concentration of 5120 μg/mL. *C. albicans* ATCC 10231-standard strain was streaked into Sabouraud dextrose agar (SDA) medium using the quadrant streak plate technique. The inoculated SDA plate was incubated for 24 at 37 °C. The inoculum was adjusted to 1×10^6 CFU/ml by measuring absorbance in a spectrophotometer at a wavelength of 530 nm or by matching a turbidity equivalent to 0.5 M McFarland reagent. The swab was dipped into inoculum. The dipped swab was spread well into the Mueller–Hinton agar plate supplemented with 2% glucose. Three cups were made in the inoculated plates by using cork pourer. Aliquot of 100 μL (512 μg/mL) of the tested compound was dispensed into the cup and 100μ L of negative control DMSO solution was added in another cup. Fluconazole (30 μg) disc was applied as the standard positive controls for and anticandidal activity. Finally, the plates were incubated aerobically at 37 °C for 24 h. After the incubation time, the results recorded by measuring the zone of inhibition (mm) by aid of ruler. The antifungal assay was carried out in triplicate and the mean value was calculated.

2.2.2. MIC

The MIC for benzoquinazoline compounds was determined using the broth dilution method according to the Clinical and Laboratory Standards Institute (CLSI) guidelines (Wayne, PA 2017). In a 7 mL screw capped sterile tube, 1 mL of Roswell Park Memorial Institute (RPMI) 1640 medium was dispensed. Fourteen RPMI 1640 tubes were used for each compound and labelled from one to 14. Stock solution of each compound was dissolved in DMSO to obtain concentration of 4096 μg/ml. One mL of stock solution (4096 μg/ml) was transferred by automatic pipette to the first RPMI 1640 tube to obtain 2-fold dilution. The contents were mixed well by pipetting up and down several times. Then 1 mL of the first tube was transferred into the second tubes and the contents were mixed well. The procedure was repeated to the twelfth RPMI 1640 tube and one mLof this tube was discarded. *C. albicans* ATCC 2091 was used standard strain. The standard strain was cultured in SDA plate for 24 hour at 37 °C. After the incubation period, three to five pure colonies of *C. albicans* ATCC 2091 was suspended and homogenized in RPMI 1640 broth by vigorous shaking. The suspension was adjusted to 1×10^6 CFU/ml by measuring absorbance in a spectrophotometer at a wavelength of 530 nm. The adjusted suspension was diluted in RPMI 1640 broth to obtain working inoculum (1×10^3 CFU/ml). One mL of diluted suspension was dispensed in each tube to obtain the recommended inoculum (0.5×10^3 CFU/ml) except the fourteenth tube which used as positive control to check the sterility of the medium. The tube number 13 was used as negative control to check the support of the medium to grow the inoculated yeast. Fluconazole used as standard control as antifungal. All tubes were incubated at 37 °C for 24 h. After the incubation period, the MIC results were recorded manually.

2.3. Docking method

Molecular operating environment (MOE) software (Montreal, QC, Canada) was used in this study. The 5tz1 (VT-1161) crystal

structure of CYP51 make sterol 14 α -demethylase is used to study the binding modes between the docked-selected compounds and amino acid residues in the active site of CYP51 sterol 14 α-demethylase. The CYP51 sterol 14 α-demethylase protein structure was got from the Protein Data Bank [PDB Code 5tz1] (Hargrove et al., 2017). The structures of the synthesized and reference compounds were constructed using MOE-Builder. The related 3D structures also obtained, and the energies of the identified molecules are minimized using the default parameters of MOE energy minimization algorithm. From the result of docking, 10 conformations were produced as the maximum allowed for each ligand using the default parameters of MOE (placement, triangle matcher; rescoring 1, London dG; refinement, force field; rescoring 2, (GBVI/WSA ΔG)) (Hargrove et al., 2017). The 300 top-ranked conformations of the docked compounds were saved in a separate database.

2.4. QSAR method

The structures of these substances were depicted using the molecular builder module of MOE software (version 2015.10). Then, they minimized their energy by employing the steepest descent, conjugate, and truncated Newton methods. Applying the MMFF94 model as a force field and setting the energy tolerance threshold to 0.01 kcal/mol for the root mean square gradient. A stochastic technique was employed to determine the conformation of an energy-minimized structure. The relative pMIC value of each compound was manually entered into the database alongside each molecule. Calculated from the log of the octanol/water partition coefficient using an eight-parameter model, the physical–chemical property descriptor known as h log P was derived from this value.

Hueckel Theory model (Labute P. 2008); Log(o/w) represents the log of the octanol/water partition coefficient (including implicit hydrogen); SlogP represents the log of the octanol/water partition coefficient, and SlogP VSA9 may be defined as the sum of van der Waals surface area (vi) such that the contribution to logP(o/w) for atom as calculated in the SlogP descriptor (Li) is in the range (>0.40) divided by the total surface area; SMR is the descriptor of molecular refractivity and SMR_VSA7 can be defined as the sum of van der Waals surface area (vi) such that molecular refractivity (Ri) is in the range (>0.56) divided by the total surface area (Bian et al. 2017, Abuelizz et al., 2020c).

3. Result and discussion

3.1. Chemistry

According to previously published procedures **(**Al-Salahi et al., 2015, 2018a, 2019a; Abuelizz et al., 2020a and 2020b), 3-ethyl(phenethyl)-2-thioxobenzo[*g*]quinazolines (**1**&**2**) are generated in high yields via the reaction of ethyl(phenethyl)isothiocyanate with 3 amino-2-naphthaoic acid in DMF under refluxing conditions for 3–5 h **(**Scheme 1**)**. The S-alkylated benzo[*g*]quinazolines **3–5** were obtained by reacting benzo[*g*]quinazolines **1** and **2** with the appropriate alkyl(heteroalkyl)halides in the presence of potassium carbonate at 90 °C for 20 h. Hydrazinolysis of **1** in boiling DMF for 15–18 h gave **c**ompound **6**. Using NMR and MS analyses, the structures of compounds **1**–**6** are confirmed. Observing the three pairs of aromatic proton resonances in the range of 8.8–7.5 ppm proved the benzoquinazoline core of molecule. Whereas in case of ^{13}C NMR, the 2-thioxo group appeared at 175.4 ppm for **1** and **2**. The protons of *N*-ethyl in **1** are assigned as triplet and quartet at 1.27 and 4.49 ppm while in ^{13}C NMR spectrum they appeared at 12.7 and 41.4 ppm. The -*S*-piperdinoethyl (**4**) protons resonances are observed in the range 4.13–1.28 ppm **(**Al-Salahi et al., 2018a, 2019a; Abuelizz et al., 2020b). The hydrazino compound (**6**) is confirmed through two characteristic singlets at 9.60 and 6.25 ppm for –NH-NH_2 (Abuelizz et al., 2020a). A singlets of two protons were assigned at 5.35 and 4.62 ppm. for CH_2– of the benzyl-moiety in the case **3** and **5.**

3.2. Anticandidal activity

Previous research on benzoquinazoline derivatives and their antifungal properties (Abuelizz et al., 2021) revealed that the benzo[*g*]quinazoline platform might be utilized as a scaffold for the further construction of novel derivatives with a robust anticandidal effect, in particular against the *C. albicans* strain. The fact that the conjugation of 2-S-benzyl/OMe-benzyl and 3-N-benzyl/butyl substituents (Fig. 1**A**) to the benzoquinazoline unit has demonstrated a good activity against candidiasis has already been discussed by our research group (Abuelizz et al., 2021). In this setting, the benzo[*g*]quinazolines **1**–**6** were tested *in vitro* against *C. albicans*, and their MIC values were determined using the colorimetric broth microdilution technique. The results were compared to fluconazole, the standard drug, and the computed MIC was reported in μg/mL. In this study, we anticipated that the adjacent conjugation of 2-S-(CN-benzyl, benzyl, and ethyl piperidinyl) and 3-N-ethyl/phenethyl substituents to the benzo[*g*]quinazoline scaffold could be an effective anticandidal combination (Fig. 1**B**). The activities of benzo[g]quinazolines **1**–**6** against the investigated *C. albicans* strain ranged from moderate to high, as shown in Table 1. Compounds **1** and **2** showed the highest inhibition zone (20 & 22 mm) in regards to fluconazole (26 mm), whereas compounds **3**–**6** showed good inhibition zones (15–18 mm). As shown in Table 1, the greatest activity of parents **1** and **2** was considerably influenced by the presence of a thioxo group; however, its chemical transformation into thioalkyl (**3**–**5**) or hydrazine (**6**) derivatives did not have a positive effect on the activity profile. In general, it is known that the electron displacements (e.g. Inductive, ±I and/or Resonance, ±R effects), caused by electron withdrawing/donating groups, significantly affect the antifungal activity as shown by compound **3** (inhibition zone = 18 mm), which attributed to the CN as electron withdrawn group and its expected role in the binding effect at active site of the enzyme. On the basis of the chemical transformation of the parent benzo[*g*] quinazolines **1, 2** scaffold, the S-alkylated derivatives **3**–**5** and the hydrazine derivative **6** are created with different anticandidal effects. However, the substitution with a CN-benzyl moiety in compound **3** exhibited the best activity compared to compounds **4** and **5**. The identification of the probable target for the benzo[*g*]quinazoline's mechanism of action will precede the clarification of such structure activity relationship-related modifications.

3.3. Docking study

Docking study and biological assays were employed to identify the molecular targets of the under investigated compounds. The efforts are focused on lanosterol 14- α demethylase enzyme which consider as the main target for antifungal drugs. Moreover, Hargrove et collaborators (Hargrove et al., 2017) think that the rigidity of the substrate-binding cavity makes the P450 enzyme unique across phylogenies and the B′-helix/BC-loop (CYP51) is the most interacting area with the sterol substrate's -surface (Hargrove et al., 2012). Deduction of the probable mechanism action of benzo[g]quinazolines with antifungal activity was performed by docking study. MOE software (MOE-2015) was utilized to investigate the interactions (H- and hydrophobic bonds) of the targets and the confirmed pose with the lowest binding affinity was stored in the format of PDB. In this work, a docking study was conducted between benzo[*g*]quinazoline derivatives **1**–**6** and *Candida* spp.

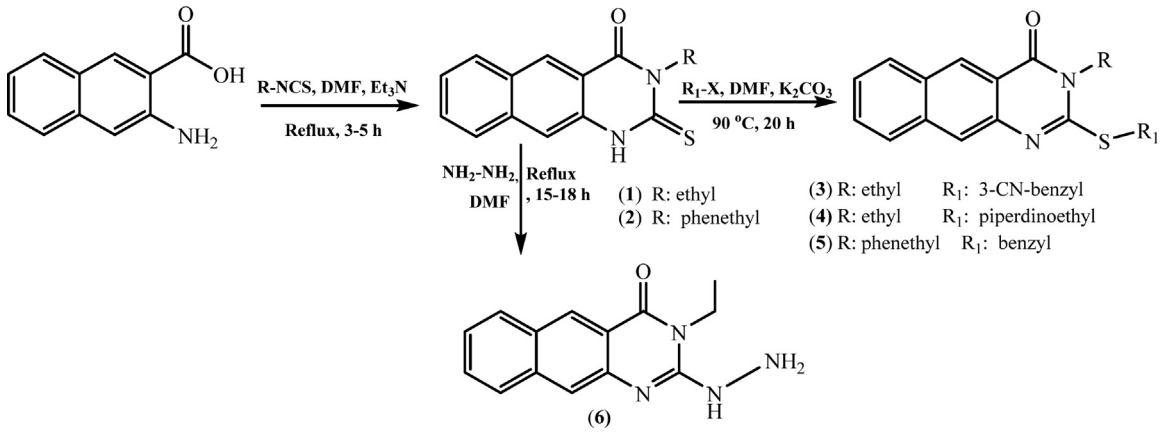

Scheme 1. The synthetic routes for benzo[g]quinazolines 1–6.

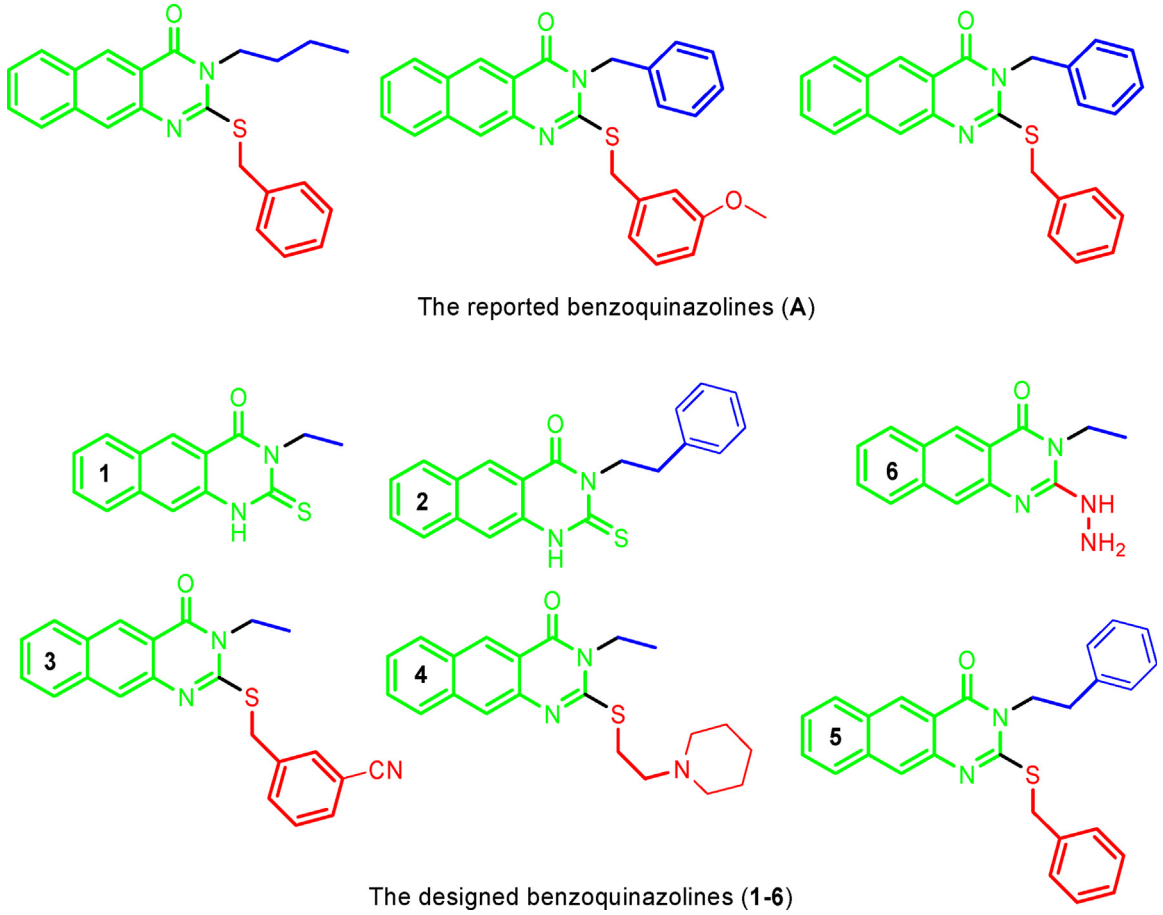

Fig. 1. (A & B). The reported and designed benzo[g]quinazolines. Green color shows the main scaffold; blue color substitution on the position 3; red color substitution on the position 2.

Table 1
The anticandidal activity of benzo[g]quinazolines **1–6.**

Compounds	Zone Inhibition (mm)	MIC (μg/ml)
1	20	256
2	22	128
3	18	128
4	16	128
5	15	128
6	15	128
Fluconazole	26	2

CYP51 to determine the binding mode of these compounds and to compare them with fluconazole and VT-1161 as reference drugs. According to the obtained results, both the synthesized benzo[g] quinazolines and reference compounds bind to the active site of *Candida* spp. CYP51 in the same manner. Docking the VT-1161, which is co-crystallized with lanosterol 14 α-demethylase, validated the docking protocol. According to MOE's findings, the chemicals' interactions with the heme iron via the thiol group serve as the primary molecular factor in inhibiting CYP51's activity (Fig. 2). Rather than the tail protruding into the cavity between

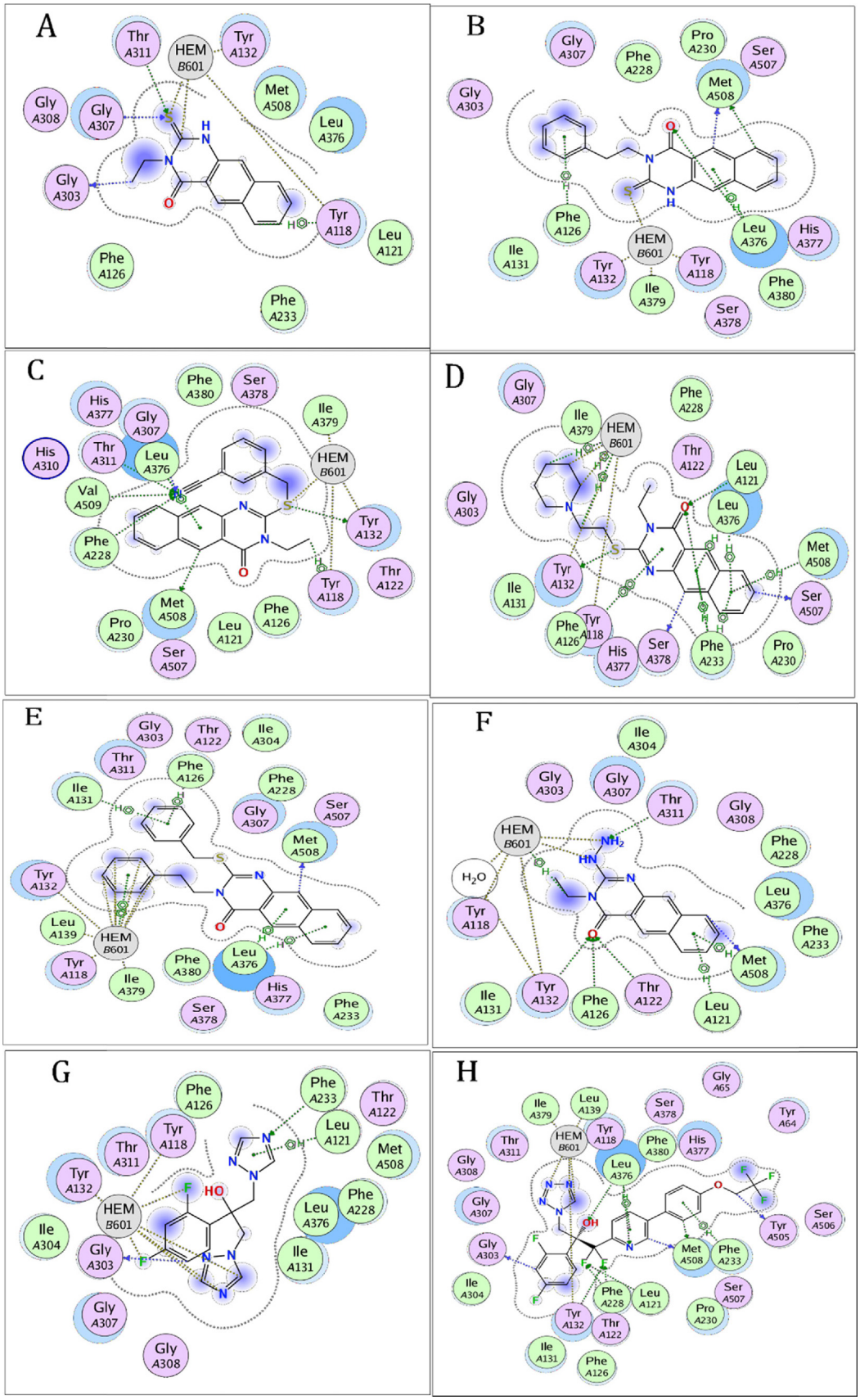

Fig. 2. 2D interactions between C. albicans against benzo[g]quinazolines **(A-F)** and references compounds fluconazole and (VT-1161 (**G, H**)).

Table 2
Docking energy, docking affinity and interactions of benzo[*g*]quinazolines **1**–**6** and references drugs with ligands.

Comp.	Ligand	Receptor	Interaction	Distance	E (kcal/mol)	Binding affinity (kcal/mol)	Heat of formation Kcal/mol
1	C 25	O GLY 303 (A)	H-donor	2.71	−0.1	−6.03	27.77
	S 30	CA GLY 307 (A)	H-acceptor	2.78	−0.1		
	S 30	CG2 THR 311 (A)	H-acceptor	3.4	−0.2		
	S 30	FE HEM 601 (A)	Metal- acceptor	3.21	≈0		
	C 7	6-ring TYR 118 (A)	H-pi	2.75	−0.3		
2	C 4	O MET 508 (A)	H-donor	2.61	−0.1	−7.16	55.85
	C 7	CBA HEM 601 (A)	H-donor	3.38	−0.1		
	O 1	CD2 LEU 376 (A)	H-acceptor	2.91	−0.1		
	S 40	CBA HEM 601 (A)	H-acceptor	2.82	−0.1		
	6-ring	CE2 PHE 126 (A)	pi-H	3.89	−0.2		
	6-ring	CD2 LEU 376 (A)	pi-H	2.95	−0.2		
	6-ring	CD2 LEU 376 (A)	pi-H	3.35	−0.2		
3	S 12	OH TYR 132 (A)	H-donor	3.33	−0.4	−8.16	88.78
	C 42	SD MET 508 (A)	H-donor	3.31	−0.1		
	N 25	CE2 PHE 228 (A)	H-acceptor	3.06	−0.2		
	N 25	CG2 THR 311 (A)	H-acceptor	2.91	−0.2		
	S 12	CBA HEM 601 (A)	H-acceptor	3.56	−0.1		
	N 25	CA GLY 307 (A)	H-acceptor	3.78	−0.1		
	N 25	CG1 VAL 509 (A)	H-acceptor	3.98	−0.1		
	C 7	6-ring TYR 118 (A)	H-pi	2.70	−0.4		
	6-ring	CD1 LEU 376 (A)	pi-H	2.97	−0.2		
	6-ring	CD2 LEU 376 (A)	pi-H	3.30	−0.2		
4	S 12	OH TYR 132 (A)	H-donor	3.63	−0.2	−8.15	13.40
	C 37	O SER 378 (A)	H-donor	2.37	−0.2		
	C 44	O SER 507 (A)	H-donor	3.38	−0.1		
	O 1	CD1 LEU 121 (A)	H-acceptor	3.23	−0.1		
	O 1	CZ PHE 233 (A)	H-acceptor	3.81	−0.1		
	C 32	FE HEM 601 (A)	Metal acceptor	3.97	≈0		
	6-ring	CE2 PHE 233 (A)	pi-H	4.74	−0.1		
	6-ring	CE2 PHE 233 (A)	pi-H	4.53	−0.1		
	6-ring	CZ PHE 233 (A)	pi-H	4.45	−0.1		
	C 16	5-ring HEM 601 (A)	H-pi	3.54	−0.2		
	C 26	5-ring HEM 601 (A)	H-pi	3.68	−0.2		
	6-ring	CD2 LEU 376 (A)	pi-H	3.83	−0.4		
	6-ring	CD2 LEU 376 (A)	pi-H	3.43	−0.3		
	6-ring	CA MET 508 (A)	pi-H	4.72	−0.2		
	6-ring	6-ring TYR 118 (A)	pi-pi	3.85	0		
5	C 39	O MET 508 (A)	H-donor	3.3	−0.1	−9.07	81.76
	6-ring	CE2 PHE 126 (A)	pi-H	3.81	−0.1		
	C 15	FE HEM 601 (A)	Metal- acceptor	2.87	≈0		
	6-ring	CD1 ILE 131 (A)	pi-H	3.61	−0.3		
	6-ring	CD1 LEU 376 (A)	pi-H	3.22	−0.2		
	6-ring	CD2 LEU 376 (A)	pi-H	3.82	−0.3		
	6-ring	CD2 LEU 376 (A)	pi-H	2.84	−0.3		
	6-ring	5-ring HEM 601 (A)	pi-pi	3.98	−0.1		
	6-ring	5-ring HEM 601 (A)	pi-pi	3.95	−0.1		
6	C 22	O MET 508 (A)	H-donor	2.81	−0.2	−6.39	37.68
	O 1	CG2 THR 122 (A)	H-acceptor	3.13	−0.1		
	O 1	CE2 PHE 126 (A)	H-acceptor	2.85	−0.1		
	O 1	CE2 TYR 132 (A)	H-acceptor	2.59	−0.1		
	N 14	CG2 THR 311 (A)	H-acceptor	2.92	−0.2		
	N 12	FE HEM 601 (A)	Metal- acceptor	3.55	≈0		
	N 14	FE HEM 601 (A)	Metal- acceptor	3.01	≈0		
	C 4	5-ring HEM 601 (A)	H-pi	2.74	−0.2		
	6-ring	CG LEU 121 (A)	pi-H	3.25	−0.1		
	6-ring	CE MET 508 (A)	pi-H	2.59	−0.3		
Fluconazole	C 28	O GLY 303 (A)	H-donor	2.57	−0.2	−7.07	13.29
	N 15	CZ PHE 233 (A)	H-acceptor	2.97	−0.2		
	F 31	CMD HEM 601 (A)	H-acceptor	3.97	−0.1		
	F 34	CBD HEM 601 (A)	H-acceptor	3.08	−0.1		
	N 22	FE HEM 601 (A)	Metal- acceptor	2.72	≈0		
	5-ring	CG LEU 121 (A)	pi-H	3.44	−0.3		
VT-1161	CBC 5	O TYR 505 (A)	H-donor	2.73	−0.1	−10.82	−237.34
	CBI 12	SD MET 508 (A)	H-donor	3.18	−0.3		
	CBJ 20	O MET 508 (A)	H-donor	2.53	−0.3		
	CAN 46	O GLY 303 (A)	H-donor	2.56	−0.2		
	NBK 22	CD2 LEU 376 (A)	H-acceptor	3.18	−0.1		
	FAR 29	CD1 LEU 121 (A)	H-acceptor	3.16	−0.1		
	FAR 29	CZ PHE 228 (A)	H-acceptor	2.59	−0.1		
	FAS 30	CG2 THR 122 (A)	H-acceptor	2.94	−0.1		
	FAS 30	CE2 TYR 132 (A)	H-acceptor	2.41	−0.1		
	OAA 41	CD1 LEU 376 (A)	H-acceptor	2.92	−0.1		

Table 2 (*continued*)

Comp.	Ligand	Receptor	Interaction	Distance	E (kcal/mol)	Binding affinity (kcal/mol)	Heat of formation Kcal/mol
	NAF 38	FE HEM 601 (A)	Metal-acceptor	2.48	≈0		
	6-ring	CE2 PHE 233 (A)	pi-H	3.46	−0.1		
	6-ring	CD2 LEU 376 (A)	pi-H	3.565	−0.1		
	CBC 5	O TYR 505 (A)	H-donor	2.73	−0.1		
	5-ring	6-ring TYR 118 (1)	pi-pi	3.73	−0.1		

the heme and the residues Ile131, Tyr132, and Gly303, as was previously thought to be the case, the benzo[g]quinazolines ring occupied the small channel leading to the active site entrance. Further to interacting with lipophilic residues like Leu376, Phe380, and Met508 through - interactions, naphthalene moiety also interacts with Tyr118. As presented in Table 2, benzo[g]quinazoline 5 exhibited the greatest activity, hence, docked pose analysis was performed to determine the interactions that may be responsible for the inhibition of lanosterol 14α-demethylase. Compound 5 with a docking affinity of −9.07 showed two hydrogen bonds one with TYR132, the second with HEM601 through the bridge of water molecule, besides, one pi-cation interactions with iron ion of HEM601, as well as, six hydrophobic interactions (pi–pi) with HEM601, PHE233, PHE126, TYR118, and HIS377 as shown in Table 2 and Fig. 2. Furthermore, hydrophobic interactions (Pi-alkyl) with residues ILE131, HEM601, LEU376, and MET508 have shown. On the other hand, benzo[g]quinazoline **4** (docking affinity = -8.15) has two hydrogen bonds with TYR132 and TYR118, three Pi-Pi interaction with TYR118, and HIS377, as well as, alkyl interaction with HEM601, and LEU376, pi-alkyl interaction with TYR118, TYR132, HEM 601, LEU376, MET508, as shown in Fig. 2. The VT-1161 is showing coordination bond with HEM601, one hydrogen bond with HIS377, and three pi–pi interactions with TYR118, PHE233, and HIS377 (Fig. 2). Comparison of docked pose of compounds **4**, **5** and VT-1161 showed that there are three common interacting residues, namely TYR118, HIS377, and PHE233. These common interactions supported that inhibition of lanosterol 14α-demethylase considered the antifungal activity reason of synthesized benzoquinazolines. Furthermore, all compounds have hydrophobic interactions with heme group, as well as compounds **1**, **6**, fluconazole, and VT-1161 form pi-cation interactions with the iron ion of HEM601, which gives strong evidence for the activity of these compounds against fungal. As reported previously (Devgun, et al. 2021), alteration on drug accumulation in the cell via a change in lanosterol demethylase (Erg11p) and ergosterol biosynthesis (target of drug), resulted the resistant mechanism against fluconazole in *C. albicans*. Thus, the sterol 14 α-demethylase protein (PDB: 5TZ1) represents the main goal in the antifungal treatment strategy. The binding energy, interactions and binding affinity (kcal/mol) of benzo[g]quinazolines are calculated and presented in Table 2. The obtained data showed good correlation between the scores and the antifungal effects of the targets. Based on the results of anticandidal activity, 2D interactions of benzo[g] quinazolines **1**–**6**, fluconazole as well as are constructed (Fig. 2).

3.4. QSAR

QSAR analysis was performed to further explore the discovered pharmacological characteristics and to determine the primary regulating elements controlling the activities. In this study, we used a dataset gathered from the literature that contained 69 molecules including the synthesized benzo[g]quinazolines. The 69 compounds were divided into two groups: a training set (56) and a test set (13) using Kennard–Stone algorithm (Kennard and Stone 1969). For each molecule, a SMILES string was constructed (Tables S1 & S2 and Fig. S1) (Abuelizz et al., 2020a). The test set complied with the requirements that have at least five compounds with structures and activities that span the structures and activities range existed in the set of training. The activity was quantified using the pMIC method (pMIC = -log (MIC 10^{-6}), where MIC is reported in (μg/mL) and was converted to Molar (M) to calculate MIC of anticandidal drug. For sketching the benzo[g] quinazolines structures, the molecular builder module of MOE software (version 2015.10) was applied and the QSAR model was created by using AutoQSAR. For the training data set, regression analysis was done, and the quality was assessed using the squared correlation coefficient (r^2), root mean square error (RMSE) (Stewart, 1989), and cross validation squared correlation coefficient q^2 (Hargrove et al., 2012). The q^2 value is used to assess the QSAR model's prediction performance and stability (Takahashi et al., 2010). Subdivided surface

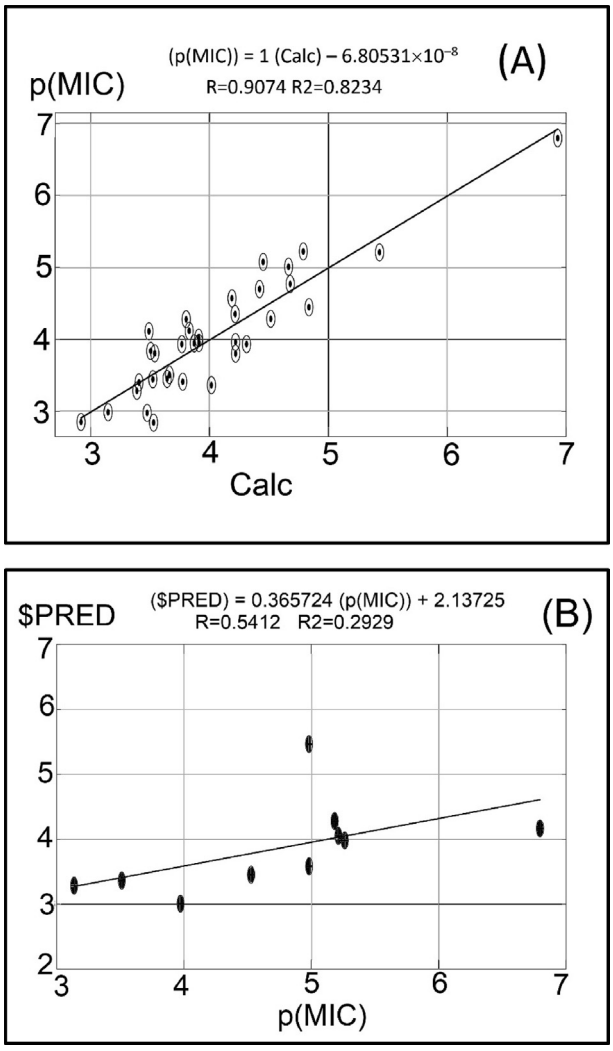

Fig. 3. The correlation plot between experimental and the predicted pMIC values of compounds from (A) training set and (B) test set.

areas such as descriptor PEOE_VSA + 5, PEOE_VSA-5, Q_VSA_POL and PEOE_VSA_POS can be defined as the sum of van der Waals surface area (vi) such that partial charge (qi) is in the range ([0.00,0.05), [−0.25, −0.20) and less than −0.30, respectively) divided by the total surface area.

$$\begin{aligned} p(MIC) = {} & 2.47969 - 0.04222 \times (PEOE\_VSA + 5) + 0.04984 \\ & \times (PEOE\_VSA - 5) + 0.00909 \times (PEOE\_VSA\_POS) \\ & - 0.00794 \times (Q\_VSA\_POL) + 0.01352 \\ & \times (SMR\_VSA1) \end{aligned} \quad (1)$$

n = 5, r^2 = 0.82338, RMSE = 0.33864, q2 = 0.75174.

Biological features and statistical methods were applied in conducting process of the 2D QSAR for benzoquinazoline derivatives analyses. A method for identifying outliers based on the "leave-one-out" (LOO) cross-validation coefficient (q^2) was described and successfully applied. An optimum QSAR equation with eight parameters (n = 5) exhibited acceptable statistical quality in both regression (R^2 = 0.82338) and "LOO" cross-validation (q^2 = 0.75174) was derived (Chen et al., 2008). The predicted pMIC values for the training and test sets were plotted against the practical values. The obtained predicted pMIC results for the modeling set were in good agreement with the practical outcomes for anticandidal activity. As shown in Eq. (1) and Fig. 3, the model revealed a strong correlation between observed and predicted activity, with R^2 = 0.82338 and q^2 = 0.75174. Following that, the model was used to validate the test set and accurately predicted the activity of the test set compounds with a r^2 value of 0.5412. (Fig. 3). Other descriptors (including SMR_VSA1) suggested that dipole_moment played a role in the anticandidal activity action of these benzoquinazolines.

4. Conclusion

The Cup-plate diffusion method was used to assess the *in vitro* activity of benzo[*g*]quinazolines **1–6** against *C. albicans* ATCC 10231. The results showed that the target compounds had good anticandidal activity, with compounds **1** (inhibition zone = 20 mm) and **2** (inhibition zone = 22 mm) in comparison to fluconazole (inhibition zone = 26 mm). Compounds **4** and **5** yielded good results in silico (their docking affinities are −8.15 and −9.07 kcal/mol with respect to fluconazole and VT-1161, respectively; these values are also consistent with the compounds' anticandidal activities). In addition, we found that TYR118, HIS378, and PHE233 are all interacting residues in the docked poses of VT-1161, compounds **4**, and **5**. With a calculated r^2 = 0.82338 and q^2 = 0.75174, the QSAR investigation demonstrated a good correlation between observed and anticipated activity in the validation model.

Funding

This work was funded by Researchers Supporting Project, King Saud University, Riyadh, Saudi Arabia through grant number RSPD2023R566.

Institutional Review Board Statement

Not applicable.

Informed Consent Statement

Not applicable.

Sample Availability

Samples of the compounds **1–6** are available from the authors.

CRediT authorship contribution statement

Hatem A. Abuelizz: Conceptualization, Writing – original draft, Data curation. **Ahmed H. Bakheit:** Data curation. **Mohamed H. Al-Agamy:** Methodology, Data curation. **Harunor Rashid:** Writing – review & editing. **Gamal A.E. Mostafa:** Writing – review & editing. **Rashad Al-Salahi:** Conceptualization, Writing – original draft, Investigation, Data curation, Supervision.

Declaration of Competing Interest

The authors declare that they have no known competing financial interests or personal relationships that could have appeared to influence the work reported in this paper.

Acknowledgments

The authors extend their appreciation to the Researchers Supporting Project, King Saud University, Riyadh, Saudi Arabia for funding this work through grant number RSPD2023R566.

Appendix A. Supplementary material

Supplementary data to this article can be found online at https://doi.org/10.1016/j.jsps.2023.04.012.

References

Abuelizz, H.A., El-Dib, R.A., Marzouk, M., Al-Salahi, R., 2018. In vitro evaluation of new 2-phenoxy-benzo[g][1,2,4]triazolo[1,5-a]quinazoline derivatives as antimicrobial agents. Microb. Pathog. 117, 60–67.

Abuelizz, H.A., Marzouk, M., Bakheit, A.H., Al-Salahi, R., 2020a. Investigation of some benzoquinazoline and quinazoline derivatives as novel inhibitors of HCV-NS3/4A protease: Biological, molecular docking and QSAR studies. RSC Adv. 10, 35820–35830.

Abuelizz, H.A., Marzouk, M., Bakheit, A.H., Awad, H.M., Soltan, M.M., Naglah, A.M., Al-Salahi, R., 2020b. Antiproliferative and Antiangiogenic Properties of New VEGFR-2-Targeting 2-Thioxobenzo [g] Quinazoline Derivatives (In Vitro). Molecules 25, 5944.

Abuelizz, H.A., Awad, H.M., Marzouk, M., Nasr, F.A., Bakheit, A.H., Naglah, A.M., Al-Shakliah, N.S., Al-Salahi, R., 2020c. Exploiting the 4-Hydrazinobenzoic acid moiety for the development of anticancer agents: Synthesis and biological profile. Bioorg. Chem. 102, 104098.

Abuelizz, H.A., Marzouk, M., Bakhiet, A., Abdel-Aziz, M.M., Ezzeldin, E., Rashid, H., Al-Salahi, R., 2021. In silico study and biological screening of benzoquinazolines as potential antimicrobial agents against methicillin-resistant Staphylococcus aureus, carbapenem-resistant Klebsiella pneumoniae, and fluconazole-resistant Candida albicans. Microb. Pathog. 160, 105157.

Almehizi, A.A., Abuelizz, H.A., Taie, H.A.A., ElHassane, A., Marzouk, M., Al-Salahi, R., 2019. Investigation the antioxidant activity of benzo[g]triazoloquinazolines correlated with a DFT study. Saudi Pharm. J. 27, 133–137.

Al-Salahi, R., El Dib, R.A., Marzouk, M., 2015. Synthesis and in vitro cytotoxicity evaluation of new 2-thioxo-benzo[g]quinazolin-4(3H)-one derivatives. Heterocycles 91, 1735–1751.

Al-Salahi, R., Abuelizz, H.A., Ghabbour, H.A., El-Dib, R., Marzouk, M., 2016b. Molecular docking study and antiviral evaluation of 2-thioxo-benzo[g] quinazolin-4(3H)-one derivatives. Chem. Cent. J. 10, 2016.

Al-Salahi, R., Abuelizz, H.A., El Dib, R., Marzouk, M., Alshammari, M.B., 2017. Antimicrobial activity of new 2-thioxo-benzo[g]quinazolin-4(3H)-one derivatives. Med. Chem. 13, 85–92.

Al-Salahi, R., A Abuelizz, H., Wadi, M., A El Dib, R., A Alotaibi, M., Marzouk, M., 2016. Antimicrobial activity of synthesized 2-methylthiobenzo [g][1, 2, 4]-triazolo [1, 5-a]quinazoline derivatives. Med. Chem. 12, 760–766.

Al-Salahi, R., Ahmad, R., Anouar, E., Iwana Nor Azman, N.I., Marzouk, M., Abuelizz, H. A., 2018a. 3-Benzyl (phenethyl)-2-thioxobenzo[g]quinazolines as a new class of potent α-glucosidase inhibitors: synthesis and molecular docking study. Future medicinal chemistry 10, 1889–1905.

Al-Salahi, R., Moustapha, M.E., Abuelizz, H.A., Alharthi, A.I., Alburikan, K.A., Ibrahim, I.T., Marzouk, M., Motaleb, M.A., 2018b. Radioiodination and biodistribution of newly synthesized 3-benzyl-2-([3-methoxybenzyl] thio) benzo [g] quinazolin-4-(3H)-one in tumor bearing mice. Saudi Pharmaceut. J. 26, 1120–1126.

Al-Salahi, R., Marzouk, M., Abuelizz, H.A., 2019a. Anti-HAV evaluation and molecular docking of newly synthesized 3-benzyl (phenethyl) benzo [g] quinazolines. Bioorg. Med. Chem. Lett. 29, 1614–1619.
Al-Salahi, R., Taie, H.A.A., Bakheit, A.H., Marzouk, M., Almehizia, A.A., Herqash, R., Abuelizz, H.A., 2019b. Antioxidant activities and molecular docking of 2-thioxobenzo[g]quinazoline derivatives. Pharmacol. Rep. 71, 695–700.
Andes, D.R., Safdar, N., Baddley, J.W., Alexander, B., Brumble, L., Freifeld, A., Hadley, S., Herwaldt, L., Kauffman, C., Lyon, G.M., 2016. The epidemiology and outcomes of invasive Candida infections among organ transplant recipients in the United States: results of the Transplant-Associated Infection Surveillance Network (TRANSNET). Transpl. Infect. Dis. 18, 921–931.
Bian, J., Li, T., Weng, T., Wang, J., Chen, Y., Li, Z., 2017. Synthesis, evaluation and quantitative structure–activity relationship (QSAR) analysis of Wogonin derivatives as cytotoxic agents. Bioorg. Med. Chem. Lett. 27, 1012–1016.
Chandrika, K.V.S.M., Sharma, S., 2020. Promising antifungal agents: A minireview. Bioorg. Med. Chem. 28, 115398.
Chen, J., Qian, L., Shen, Y., Chen, L., Zheng, K., 2008. A QSAR study and molecular design of benzothiazole derivatives as potent anticancer agents. Sci. China, Ser. B 51, 111–119.
Conti, H.R., Huppler, A.R., Whibley, N., Gaffen, S.L., 2014. Animal models for candidiasis. Curr. Protoc. Immunol. 105, 16–19.
Dadar, M., Tiwari, R., Karthik, K., Chakraborty, S., Shahali, Y., Dhama, K., 2018. Candida albicans-Biology, molecular characterization, pathogenicity, and advances in diagnosis and control–An update. Microb. Pathog. 117, 128–138.
Devgun, M., Prasad, S., Khokra, S., Narang, R., 2021. Molecular docking studies of dihydropyridazin-3 (2H)-one derivatives as Antifungal, antibacterial and anti-helmintic agents. World J. Adv. Res. Rev. 12, 186–214.
Hargrove, T.Y., Wawrzak, Z., Liu, J., Waterman, M.R., Nes, W.D., Lepesheva, G.I., 2012. Structural complex of sterol 14α-demethylase (CYP51) with 14α-methylenecyclopropyl-Δ7-24, 25-dihydrolanosterol. J. Lipid Res. 53, 311–320.
Hargrove, T.Y., Friggeri, L., Wawrzak, Z., Qi, A., Hoekstra, W.J., Schotzinger, R.J., York, J.D., Guengerich, F.P., Lepesheva, G.I., 2017. Structural analyses of Candida albicans sterol 14α-demethylase complexed with azole drugs address the molecular basis of azole-mediated inhibition of fungal sterol biosynthesis. J. Biol. Chem. 292, 6728–6743.
Kennard, R.W., Stone, L.A., 1969. Computer aided design of experimental. Technometrics 11, 137–148.
Labute, P., 2008. The generalized Born/volume integral implicit solvent model: estimation of the free energy of hydration using London dispersion instead of atomic surface area. J. Comput. Chem. 29, 1693–1698.
Nobile, C.J., Johnson, A.D., 2015. Candida albicans biofilms and human disease. Annu. Rev. Microbiol. 69, 71.
Pfaller, M.A., Moet, G.J., Messer, S.A., Jones, R.N., Castanheira, M., 2011. Candida bloodstream infections: comparison of species distributions and antifungal resistance patterns in community-onset and nosocomial isolates in the SENTRY Antimicrobial Surveillance Program, 2008–2009. Antimicrob. Agents Chemother. 55, 561–566.
Rothstein, D.M., Spacciapoli, P., Tran, L.T., Xu, T., Roberts, F.D., Dalla Serra, M., Buxton, D.K., Oppenheim, F.G., Friden, P., 2001. Anticandida activity is retained in P-113, a 12-amino-acid fragment of histatin 5. Antimicrob. Agents Chemother. 45, 1367–1373.
Stewart, J.J.P., 1989. Optimization of parameters for semiempirical methods I. Method. J. Comput. Chem. 10, 209–220.
Takahashi, J., Hijikuro, I., Kihara, T., Murugesh, M.G., Fuse, S., Kunimoto, R., Tsumura, Y., Akaike, A., Niidome, T., Okuno, Y., 2010. Design, synthesis, evaluation and QSAR analysis of N1-substituted norcymserine derivatives as selective butyrylcholinesterase inhibitors. Bioorg. Med. Chem. Lett. 20, 1718–1720.
Turner, S.A., Butler, G., 2014. The Candida pathogenic species complex. Cold Spring Harbor Perspect. Med. 4, a019778.
Wayne, P.A., 2009. Clinical and Laboratory Standards Institute. Method for antifungal disk diffusion susceptibility testing of yeasts; approved guideline, 2nd ed CLSI document M44-A2 Clinical and Laboratory Standards Institute.
Wayne, P.A. 2017. Clinical and Laboratory Standards Institute. Reference method for broth dilution antifungal susceptibility testing of yeasts, 4th ed Approved standard M27 Clinical and Laboratory Standards Institute.
Whaley, S.G., Berkow, E.L., Rybak, J.M., Nishimoto, A.T., Barker, K.S., Rogers, P.D., 2017. Azole antifungal resistance in Candida albicans and emerging non-albicans Candida species. Front. Microbiol. 7, 2173.
Yousef, T.A., Ezzeldin, E., Abdel-Aziz, H.A., Al-Agamy, M.H., Mostafa, G.A.E., 2020. Charge transfer complex of neostigmine with 2, 3-Dichloro-5, 6-dicyano-1, 4-benzoquinone: Synthesis, spectroscopic characterization, antimicrobial activity, and theoretical study. Drug Des. Devel. Ther. 14, 4115.